SEISMIC RISK ASSESSMENT OF EXISTING LIFELINES FOR URBAN RENEWAL PLANNING

T. Koike[1] and F. Mochizuki[2]

ABSTRACT

This paper describes the seismic risk assessment for existing lifelines under a deteriorating process and also discusses an optimal planning for disaster prevention preparedness. The system performance of trunk lines and distribution networks are discussed from the retrofitting strategy for structural improvement of the nodes and links. The numerical studies for existing lifelines are focused on seismically retrofit works which must be optimized efficiently under the constraint of a limited budget for urban renewal planning.

Introduction

This paper describes the seismic risk assessment for existing lifelines under a deteriorating process, and also discusses the optimal planning for disaster prevention preparedness.

Lifeline structures are always threatened, not only by a corrosive environment or third party incident risk, but also by various natural hazards including earthquake loads. After the 1995 Kobe earthquake, the design guidelines were revised and a Level 2 earthquake was specified. This new specification is larger than the seismic load of the previous code. As such, old infrastructure that was constructed before 1980, are vulnerable to future earthquakes. The seismic reinforcement of trunk lines or transmission networks of major lifeline systems is preferably adopted as the first step in seismic disaster prevention activities. However, the reinforcement of the distribution and supply networks may be delayed or postponed because there are too many vulnerable structural elements. Therefore, any seismic retrofitting is restricted by large costs when old vulnerable joints are replaced with new seismically high performance joints in buried pipes.

In view of this situation, the most cost effective method for seismic investment can be to consider the net present value of the disaster prevention project, which considers not only the restoration cost for physical damage but also the loss of social benefit and income gains due to in-serviceability of water supply. Serviceability from the supply nodes of trunk lines to demand nodes of distribution networks is probabilistically analyzed to evaluate the loss of such a social benefit under seismic risks.

Finally, the numerical studies for existing lifelines are focused on seismically retrofit works, which must be optimized efficiently under the constraint of a limited budget for urban renewal planning.

---

[1]Professor, Dept. of Civil Engineering, Musashi Institute of Technology, Tokyo, Japan
[2]Graduate student, Dept. of Civil Engineering, Musashi Institute of Technology, Tokyo, Japan

Existing Lifeline

A middle size water supply network system located in an earthquake sensitive area is selected in this study. This lifeline system was constructed 35 years ago. Main pipelines are composed of welded steel pipes, and all other lines are made of ductile cast iron pipes with mechanical joints. Inspite of daily maintenance activity, some pipelines are corroded at their surfaces while others are deteriorated at the joints. Many old cast iron pipelines installed in the past did not meet the present design guidelines, which was revised after the 1995 Hyogoken-Nanbu earthquake.

In this situation, recent maintenance works are concentrated on replacing the old cast iron pipes with newly developed ductile cast iron pipes with anti-seismic resisting mechanism. There are many node structures including reservoirs, tanks, elevated tanks, demand nodes and treatment facilities. These structures do not have enough potential strength to resist a level 2 ground motion because these structures were built using the old seismic design code. This did not comply with the new seismic load effect for the level 2 ground motion.

The water pipelines extend into seven water distribution districts as shown in Fig.1.

(1) Link configuration   (2) Node configuration

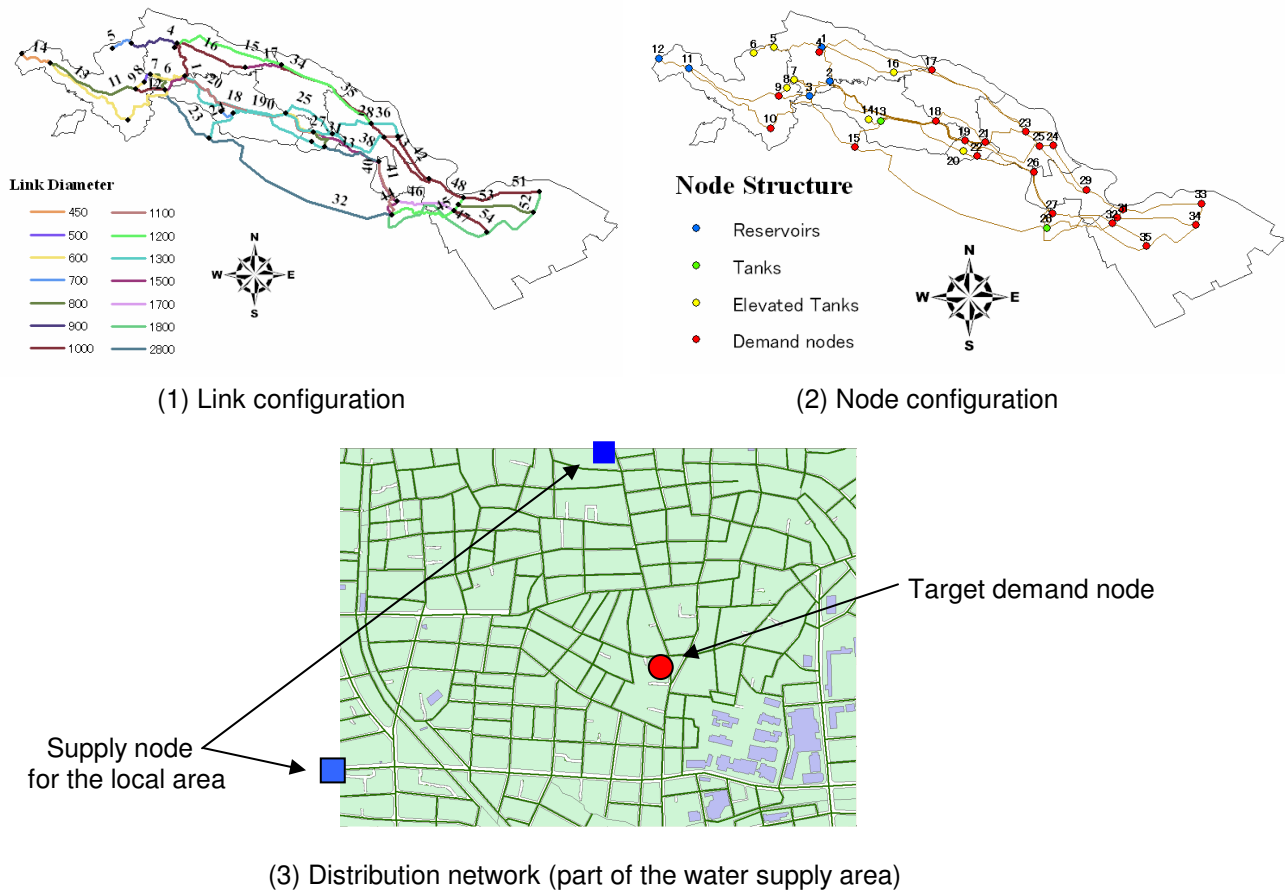(3) Distribution network (part of the water supply area)

Figure 1. Network configuration.

The nodes represent tanks, reservoirs, pumping stations and water treatment facilities as shown in Table 1. According to the managing office of this network system, the maintenance strategy for deteriorated node structures is currently being planned. The trunk lines have various pipe diameters ranging from 1700 mm to 100 mm as shown in Table 2.These lines are composed mainly of welded steel pipes.

Table 1. Facilities.

	unit
Reservoir	5
Tank	2
Elavated Tank	7
Demand node	21
Treatment facilities	3

Table 2. Pipes.

Diameter	Length (km)			
	Transmission	Distribution		
	STEEL	STEEL	DIP	CIP
1700	3.28	0	0	0
1500	2	0	0	0
1100	0.71	0	0	0
1000	199.42	0	0	0
900	2.89	0	0	0
800	67.42	0	0	0
700	2.19	0	0	0
600	39.16	295.58	41.72	5.3
500	0.65	2.06	2.49	2.1
450	1.9	0	0	0
400	0	7.39	82.03	35.71
300	0	12.76	116.3	43.11
200	0	25.65	483.5	112.08
100	0	37.13	722.13	180.28
total	319.62	380.57	1448.17	378.58

Many others are ductile cast iron pipes or cast iron pipes with mechanical joints in which a certain portion of the mechanical joints are seismically weak and old. Most typical trunk pipelines are composed of 1000mm, 800mm or 600mm diameter pipes. For the distribution lines, 600mm diameter steel pipes are widely used while small diameter pipes of 200 and 100 are mainly made of cast iron and ductile iron pipes. In this analysis, the water network system is assumed to have 3 sources, several control facilities that includes tanks, reservoirs and pumping systems, and demand nodes which can be connected to the distribution and service networks.

Seismic Performance Assessment

Structural Damage Estimation

The structural damage states for lifeline network are defined as
(a) Major damage: A structural element in the network is in the ultimate limit state
(b) Moderate damage: A structural element in the network is not in the ultimate limit state nor in the serviceability limit state.
(c) Minor damage: A structural element in the network is in the serviceability limit state.

The lifeline network system includes supply stations, transmission lines, substations and service networks to demands. These structures can be classified into two typical elements which are characterized as links and nodes. Link elements are transmission lines and distribution networks, while node elements are branch piping elements, system control facilities using valves and reservoir structures.

Link Element

Limit state for major damage mode of a link element:
$$Z_i^{major} = \delta_{cr}^{major} - \delta_i \qquad (1)$$
Limit state for minor damage mode of a link element:
$$Z_i^{minor} = \delta_{cr}^{minor} - \delta_i \qquad (2)$$
Link element can be modeled as a poly-line passing through many meshes which belong to various soil

conditions. One segment which is located in a mesh is defined as an element. In Fig.2, elements 1, 2 and 3 are located at their own meshes. Element 1 and 2 are connected at the mesh boundary.

Node Element

Limit state for major damage mode of a node structure:

$$ZN_j^{major} = \alpha_{cr}^{major} - \alpha_j \qquad (3)$$

Limit state for minor damage mode of a node structure:

$$ZN_j^{minor} = \alpha_{cr}^{minor} - \alpha_j \qquad (4)$$

The station has its own probability of failure which depends on the damage occurrences of facilities in the station system. In order to classify the undamaged node in the sense of mathematical network system from the actual damaged node, the undamaged node and fictitious sub-node are introduced and the probability of node damage can be estimated with that of the facility damage in the station.
Fig.3 is an extended node model with undamaged node and fictitious sub-nodes.
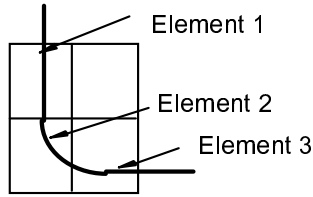

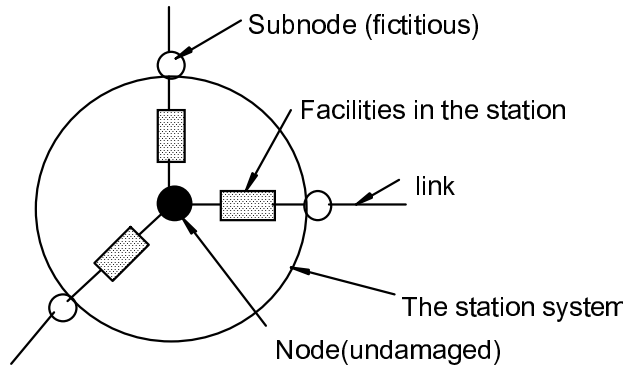Figure 2. An element model of a passing through many meshes.

Figure 3. A node model with fictitious sub-nodes.

Definition of Link and Node Damages in the Transmission Network Systems

1)Definition of Link Damage
It should be noted that a link is a series system of several line elements (i.e NL_k) connecting neighboring nodes.
Major damage of the k-th link and the j-th node:

$$E_k^{major} = \bigcup_{i=1}^{NL_k} E[Z_i^{major} < 0] \qquad , \qquad E_j^{major} = E[ZN_j^{major} < 0] \qquad (5)$$

Moderate damage of the k-th link and the j-th node:

$$E_k^{moderate} = \overline{E}_k^{major} \cap \overline{E}_k^{minor} \qquad , \qquad E_j^{moderate} = \overline{E}_j^{major} \cap \overline{E}_j^{minor} \qquad (6)$$

Minor damage of the k-th link and the j-th node:

$$E_k^{minor} = \bigcap_{i=1}^{NL_k} E[Z_i^{minor} > 0] \qquad , \qquad E_j^{minor} = E[ZN_j^{minor} > 0] \qquad (7)$$

3)Definition of extended link damage
An extended link have a series system of a link, station and a sub-node as shown in Fig.4.
Major damage of an extended link:

$$E_{k_{ex}}^{major} = \left\{ \bigcup_{i=1}^{NL_k} E[Z_i^{major} < 0] \right\} \bigcup \left\{ E[ZN_j^{major} < 0] \right\} \qquad (8)$$
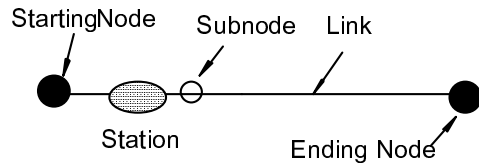
Moderate damage of an extended link:

$$E_{k_{ex}}^{\text{moderate}} = \overline{E}_{k_{ex}}^{major} \cap \overline{E}k_{ex}^{\text{minor}} \qquad (9)$$

Minor damage of an extended link:

$$E_{k_{ex}}^{\text{minor}} = \left\{ \bigcap_{i=1}^{NL_k} E\left[z_i^{\text{minor}} > 0\right] \right\} \cap \left\{ E\left[ZN_j^{\text{minor}} > 0\right] \right\} \qquad (10)$$

Figure 4. An extended link model

Fragility Curves

Structural damage for a given seismic load is often estimated using a fragility curve. The fragility curve must be furnished for two different limit states, serviceability limit state and ultimate limit state. The major damage mode can be defined as the state that the seismic load exceeds the critical strength of the ultimate limit state. The fragility curve for the major damage mode is given by

$$p_f\left(D_{major} \middle| s\right) = P\left[R^{major} - S < 0 \middle| S = s\right] \qquad (11)$$

The minor damage mode, on the other hand, is defined as the state that the seismic load is less than the critical strength of the serviceability limit state.
So the fragility curve for minor damage mode is expressed by

$$p_f\left(D_{\text{minor}} \middle| s\right) = P\left[R^{\text{minor}} - S > 0 \middle| S = s\right] \qquad (12)$$

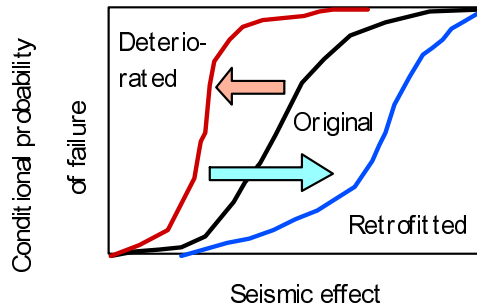The moderate damage mode is the set which does not belong to both major and minor damage modes.

Figure 5. Fragility curves for original, deteriorated and retrofitted states.

Pipes

The probability of damage states for buried pipelines under wave effect can be estimated as the probability of occurrence that the structural strain exceeds the critical pipe strain for its own limit state. Fig.6 is an example of fragility curve, in which one curve (shown as moderate) gives a boundary between the minor and moderate damages, while the other curve (shown as major) provides a boundary between the moderate and major damages.
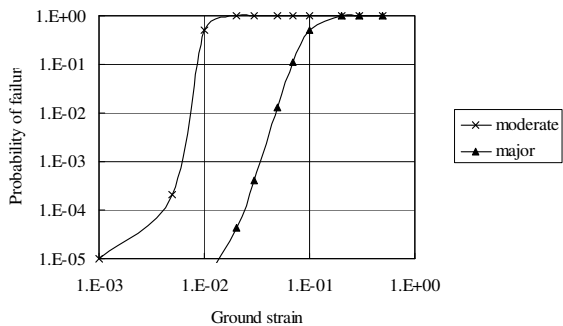

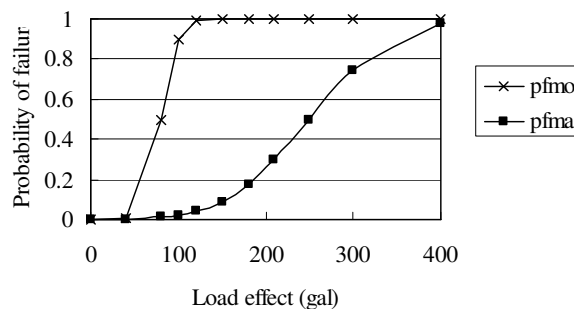Figure 6. Fragility curve of a pipe for wave effects.

Figure 7. Fragility curve for a tank.

Node Structures

Water storage steel tanks serve to control any sudden changes of water demands at several nodes of the network. When an earthquake occurs, a tank may vibrate according to two typical modes; one is the sloshing mode for longer typical period, while the other is the vibration mode for shorter one. Since water tanks are often located on the hillside, the vibration mode is more significant than the sloshing mode.

When a tank shakes at the foundation, it rotates at its center so half of it is lifted, while the other half is resisted by the soil beneath it. The base steel plate will elongate to the plastic region after exceeding the yield strain limit. So the failure criterion can be given by crack initiation from the base plate as major damage mode, while the buckling of the side wall at the lowest level is defined as the moderate damage mode. So the probability of damage states can be given by

$$P(\text{minor damage state}) = P\left[\sigma_{cr}^{buckling} - \sigma > 0\right]$$

$$P(\text{moderate damage state}) = P\left[\sigma_{cr}^{buckling} - \sigma > 0\right] \tag{13}$$

$$P(\text{major damage state}) = P\left[\varepsilon_{cr}^{crack} - \varepsilon < 0\right]$$

in which ε_{cr}^{crack} is allowable plastic strain for low cycle fatigue failure, while $\sigma_{cr}^{buckling}$ is the fully plastic stress of the sidewall steel plate.

Connectivity of Damaged Network

Definition of Connectivity from the M-th Node to N-th Node

There are many routes from the supply nodes to the demand node when all the links are undamaged as shown in Fig.8. Even if some links are damaged, several routes can connect from both nodes. Each route is composed of a series system of links. The t-th connectivity C_t^{MN} can be defined as one of the connecting routes from the source node M to the demand node N, the total number of which is equal to NC_t. Even if some links are damaged and many connecting routes are disconnected, one may keep the connectivity unless all the links are broken. In this situation, the damaged route is defined as connectivity damage.

Definition of the t-th Connectivity Damage

Major damage of connectivity:

$$C_t^{MN}(major) = \bigcup_{s=S_t}^{NC_t} E_s^{major} \tag{14}$$

Moderate damage of connectivity:

$$C_t^{MN}(moderate) = \overline{C_t^{MN}}(major) \bigcap \overline{C_t^{MN}}(minor) \tag{15}$$

Minor damage of connectivity:

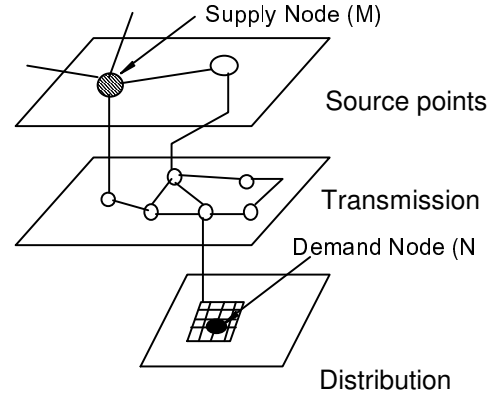$$C_t^{MN}(minor) = \bigcap_{s=S_t}^{NC_t} E_s^{minor} \tag{16}$$

Figure 8. Connectivity route model.

Definition of Probability of Connectivity Damage from Supply Node M to Demand Node N

The connectivity from supply node M to demand node N is assumed to be equal to NC set of the series system which is composed of several links.

Probability of major damage of connectivity:

$$P\left[C^{MN}(major)\right] = \bigcap_{t=1}^{NC} P\left[C_t^{MN}(major)\right] \tag{17}$$

Probability of moderate damage of connectivity:

$$P\left[C^{MN}(\text{moderate})\right] = 1 - P\left[C^{MN}(major)\right] - P\left[C^{MN}(\text{minor})\right] \tag{18}$$

Probability of minor damage of connectivity:

$$P\left[C^{MN}(\text{minor})\right] = \bigcup_{t=1}^{NC} P\left[C_t^{MN}(\text{minor})\right] \tag{19}$$

Monte Carlo Simulation is used to obtain the probability of the connectivity in the damage network. As analytical tool a transfer matrix from the supply nodes to the demand nodes is introduced, the element of which is composed from the probability p_{MN} of the supply node M to the demand node N in the damaged network.

The damage state vector A_j of the nodes after the j-th step is given by
$$A_j = H_j(\underline{D}_k)A_{j-1} \quad , \qquad j = 1, 2 \cdots, NA \tag{20}$$
where $A_o, \underline{D}_k$ and H_j are the initial damage state vector of the nodes, the k-th damage modes for all the links and the transfer matrix at the j-th step. NA is a number of steps in transferring from the source nodes to the farthest nodes.

Cost Evaluation of Seismic Retrofitting

Project Value

In assessing the viability of proposed projects, the project's financial balance or net present value (NPV) at the end of service period is measured. The project with a positive NPV is accepted, while a project with a negative NPV is rejected. So the NPV at the final stage of the project can be an important measure in assessing the risk of a proposed project. The net present value V at the service period T is defined as the summation of the social benefit B derived from the system, income gains I, daily expenditure E, initial cost C_o and maintenance costs C_M, which is given in the following formula:

$$V_o = B + I - E - (C_o + C_M) \tag{21}$$

In the private sector, the social benefit term in Eq.(21) does not apply, while public projects do not expect income gains in general. Lifeline projects, on the other hand, have both terms, because a private company has the responsibility in supplying indispensable daily services to all the customers through the lifeline network system. The income gained is used for the daily operation costs, while the social benefit is always generated by the sustainable operating system.
If a lifeline system is always threatened by seismic hazards, a disaster prevention action must be taken in order to keep the system availability with an investment C_s to the seismic reinforcement to the structural elements of the lifeline system. Then the net present value in the risk control phase can be expressed by

$$V_1 = B + I - E - (C_o + C_M + C_S) \tag{22}$$

If we can adopt the risk finance approach with the insurance premium for a business continuity plan (BCP), the net present value will be given in the following form.

$$V_2 = B + I - E - \{C_o + C_M + C_S + (C_R - Y) + mY + \alpha\} \tag{23}$$

in which m, Y, α and C_R are insurance rate, compensation money, operation fee of an insurance

company, and restoration cost after the earthquake, respectively. Since an earthquake hazard is an inevitable phenomenon in Japan, the service loss and restoration cost of the lifeline system must be taken into consideration during its service period. The net present value considering the disaster loss can be expressed by

$$V_3 = B + I - E - (C_o + C_M + C_S) - \Delta B - \Delta I - C_R \tag{24}$$

where $\Delta B, \Delta I$ and C_R are loss of benefit, loss of income, respectively.

It should be noted that the discussion on the discount rate is out of scope in this study to emphasize the effect of alternative investment strategies instead of the discount rate to the net present value.

Finally, the expected value of the project value can be obtained as follows;

$$E[V] = B + I - E - (C_o + C_M + C_S) - P[EQ](\Delta B + \Delta I + C_R) \tag{25}$$

In which $P[EQ]$ is a probability of earthquake occurrence during the service life.

When the lifeline resumes the operation, the social benefit starts. For the sake of simplicity, the amount of social benefit is assumed to be proportional to the gross domestic production (GDP). Fig.9 shows the trend of social benefit during the life cycle period.
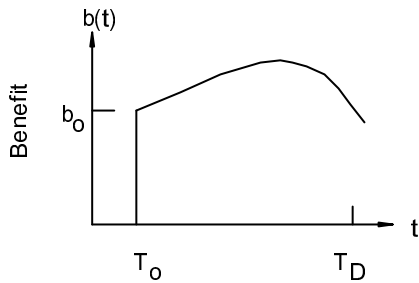

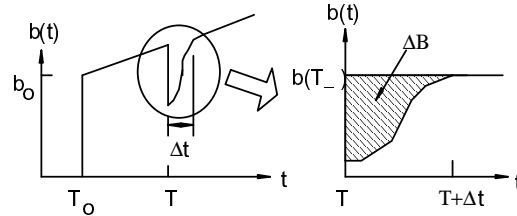Figure 9. Trend of social benefit during the life cycle period.

Figure 10. Loss of benefit under seismic damages.

The loss of benefit is shown in Fig.10 as the shaded area when an earthquake occurs at the time T and restoration process resulting from structural damages of the system resumes up to Δt.

$$b(t) \approx b_o \cdot f_D(t) \cdot \frac{GDP(t)}{GDP(T_o)} \tag{26}$$

in which b_o is a social benefit per year and is given by the ratio of $B_o/(T_D - T_o)$, while $GDP(t)$ and f_D is a degrading factor of benefit due to structural deterioration, respectively.

$$B = \int_{T_o}^{T_D} b(t) dt \quad , \quad \Delta B \approx \int_0^{\Delta t} \{b(T_-) - b(T + \tau)\} d\tau \tag{27}$$

Cost Evaluation

Damage D_k (k=minor, moderate, major) is given, the costs related to the earthquake disaster is evaluated with damage occurrence rate v, link length L_i and restoration cost per km, c_R, as follows.

$$E[C_R(D_k)] = \left\{ \sum_{i=1}^{NL} c_R(D_k) L_i v(L_i, D_k | EQ) \right\} P(EQ) \tag{28}$$

$$E[\Delta B(D_k) + \Delta I(D_k)] = \left\{ \sum_{t=1}^{NC} \{\Delta B(D_k) + \Delta I(D_k)\} P(\overline{C}_t^{MN}(D_k) | EQ) \right\} P(EQ) \tag{29}$$

1811

Numerical Study

Seismic Hazard

The lifeline system is surrounded with many potential faults. Once earthquake occurs from one of these faults, seismic wave motions will create large ground strains, while permanent ground deformation will be formed at the hazard areas of fault movement. Liquefaction induced settlement or lateral spreading and landslide may also occur although the exact location of these hazards cannot be identified.

Basically, a seismic event is a stochastic process. When a site is surrounded by several potential active faults, the probability of occurrence of the ground motion $A>a$ during the period T is given by

$$P(A > a; T) = 1 - \exp(-\nu(a)T) = 1 - \exp\left(-T\sum_i \nu_i P_i(A > a)\right) \tag{30}$$

in which ν_i is an occurrence rate of earthquake per year, and its probability from the i-th fault is given by

$$P_i(A > a) = \int_{r_o}^{r} \int_{m_o}^{m_u} F(A > a | m, r) f_{M_i}(m) f_{R_i}(r) dm dr \tag{31}$$

and $F(\ ), f(\ )$ are probability of distribution and density functions, respectively while M and R are the magnitude and epicentral distance.

When one or two earthquakes occur during its service period, this stochastic approach may provide a rational estimation of ground motion for comparatively smaller earthquakes. The probability of occurrence of a level 2 earthquake ground motion, large enough to produce inelastic responses, however is difficult to predict because of its long return period. In this case a deterministic approach or a scenario earthquake model is often adopted to predict a level 2 ground motion.

In this study, one major earthquake occurring from Tachikawa fault is adopted as a scenario earthquake, although two other major faults are located in the metropolitan area of Tokyo, Japan. Table 3 shows the fault parameters of Tachikawa fault which is located about 10 km in a north-west direction from the site.
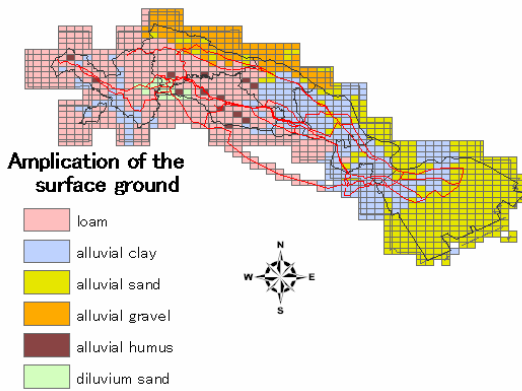

Amplication of the surface ground

- loam
- alluvial clay
- alluvial sand
- alluvial gravel
- alluvial humus
- diluvium sand

Figure 11. Amplification of the surface ground.

Table 3. Fault parameters.

Item	Symbol	Unit	Value
Magnitude	M		6.6
Length	L	km	20
Width	W	km	10
Depth	D	km	1.0
Seismic moment	Mo	dynecm	2.77×10^{25}
Direction	θ	degree	135
Slope	δ	degree	80

Surface Ground Responses

The base-rock acceleration can be evaluated with the method developed by Irikura[1] and simply modified by Harada[2]. The surface ground motions are obtained by multiplying the amplification factor derived from Fig.11 to the base-rock acceleration. Figs.12 and 13 are numerical results of ground motions when the scenario earthquake occurs. These figures suggest that the alluvial sand area shows comparatively larger ground response, while loam area represents smaller response. The liquefaction sensitive area is located at the reclamation sites of the bay area in the southern east direction.

Retrofitting Plan

Some node facilities of the trunk lines have been deteriorated, while there are many old cast iron joints in the distribution network which are vulnerable for seismic effects. In order to maintain the system connectivity from the source nodes in the trunk lines to the target demand nodes in the distribution network, one may select an appropriate reinforcing method within the same budget condition from the following two options: one is to reinforce the node facilities of trunk lines, and the second is to retrofit the link of the distribution network. Figs.14 and 15 are numerical results for this comparison in which each point corresponds to the probability of connectivity between the source nodes to the target demand nodes. In these figures, the abscissa is the probability of connectivity of the current network, while the ordinate is the probability of connectivity of the reinforced network as well as that of the initial state.
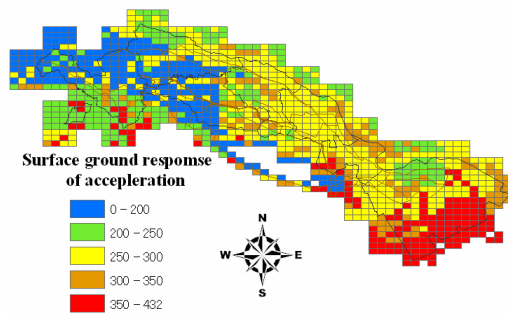

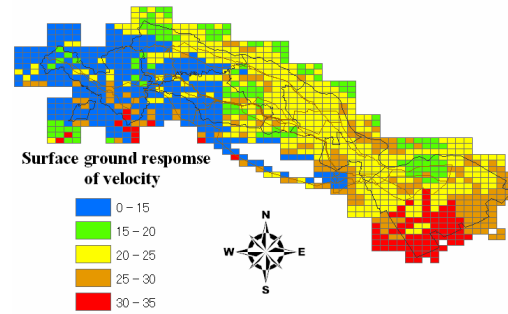Figure 12. Surface ground response of acceleration.

Figure 13. Surface ground response of velocity.

These figures suggest that the reinforcement of the nodes in the trunk lines shows diverse effects on seismic improvement, while that of the links in the distribution network is concentrated because the simple reinforcement, that all the old cast iron joints are replaced by the seismically strengthened joints, can carry out a homogeneous improvement in the distribution network system. This information will be useful to make a decision of maintenance strategies on the seismic retrofitting of the existing lifeline system.
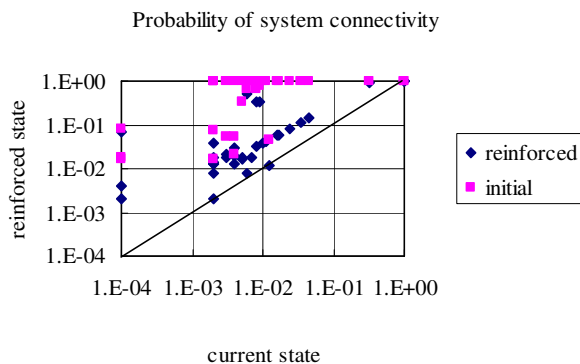

Figure 14. Reinforcing effect to the connectivity of trunk lines (30% improvement in the node resistance).
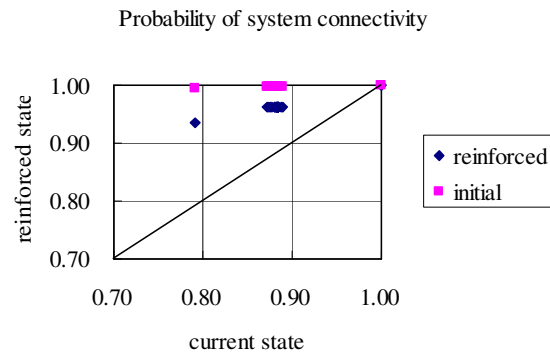

Figure 15. Reinforcing effect to the connectivity of the distribution network (30% improved in the distribution link resistance).

Conclusions

Discussions are devoted to the seismic risk assessment of existing lifelines under a deteriorating process, and also on the optimal planning for disaster prevention preparedness. The seismic risk assessment and probabilistic approaches are developed herein for the lifeline network system which is composed of trunk lines and distribution network. Numerical results suggest that the reinforcement of nodes and/or links can

improve the system connectivity. Further research will be necessary to develop the risk management and financial issues on the optimal strategies of seismic retrofitting of the existing lifeline network system under deteriorating hazard.

References

Irikura, K., 1994. Earthquake source modeling for strong motion prediction, *Seismology*, Series2, Vol.46, pp. 495-512.

Harada, T., T. Tanaka and Y. Tamura, 1995. Digital simulation of earthquake ground motions using a seismological model, *JSCE*, No.507/I-30, pp.209-217 (in Japanese).